

Analysis of Error Compensation and Design of Fine Adjustment Mechanism of Carbon-Free Car

Wang Jingdong^{1,a}, Wang Jiaqi^{1,b}, Chen Guangjun^{1,c,*}, Tang Xiang^{1,d}, Li Yan^{2,e}

¹Institute of Mechanical and Electrical Engineering, Changchun University of Science and Technology, Changchun, China

²Northeast Electric Power Design Institute CO., LTD of China Power Engineer Construction Group, Changchun, China

^a 3551086@qq.com, ^b wjqand @126.com, ^c cgjand@126.com, ^c 1723401120@qq.com, ^c 22117835@qq.com

*corresponding author

Keywords: carbon-free car, error compensation, track simulation, fine adjustment mechanism.

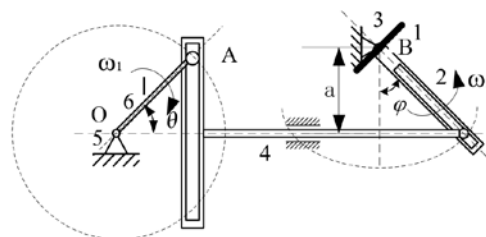
Abstract: In order to analyze the compensation relationship between adjustment quantity and track deviation, and solve the problem of high-deviation of the track, the carbon-free car whose running track approximates to a sine curve is taken as the research object. Firstly, the mathematical model of car motion is established, then the two main causes of the track deviation were concluded. By the premise that the error of departure angle is eliminated, the length of guide-bar is adjusted by screw pair to compensate the ultimate angle error of the steering shaft. Finally, the virtual prototype model of carbon-free car is established and the proper adjustment quantity is set. The experiment verifies the effectiveness and correctness of the proposed model and method.

1. Introduction

During the process of carbon-free car design, the steering mechanism is the most critical part for the obstacle avoidance function. At present, some main steering mechanisms of the carbon-free car whose running track approximates to a sine curve are slider-crank mechanism [1], crank-rocker mechanism[2], cam mechanism[3], intermittent gear mechanism[4] and so on. Their principles are easy to understand and all meet the steering requirement. But in practice, there is an obvious deviation between the running track and theoretical track which is difficult to be compensated. So it is necessary to ensure the main adjusting parameters based on the analysis and summary of the error causes and apply the corresponding adjusting mechanism to meet the design requirement.

2. Establishment of The Motion Model

The sine mechanism, which has the features of good guidance and low error [5], can turn the gyratory motion of the crack into the reciprocating linear motion of the guide bar. The kinematic diagram of the steering mechanism of the carbon-free car is shown in Fig. 1.



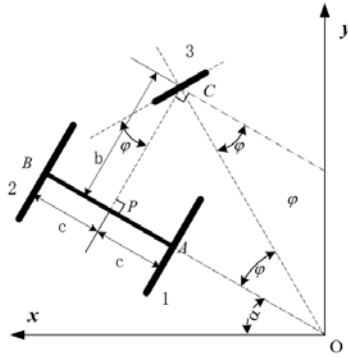
1 steering wheel 2 rocker 3 steering shaft
4 guide-bar 5 winding shaft 6 crank

Fig. 1. Kinematic diagram of the steering mechanism.

angular velocity is ω_2 , the rotation angle is φ after time t_0 , so the angle of the steering shaft is

$$\varphi(t) = \arctan\left(\frac{l \cos \theta(t)}{a}\right) \quad (1)$$

The curvature circle center of the car running track is taken as the origin and Fig. 2 is the simplified schematic diagram of running.



1 driving wheel 2 driven wheel 3 steering wheel

When the rotation angle of rocker 2 is φ in Fig. 1, the rotation angle of the steering shaft with respect to the car body is φ too in Fig. 2, and the rotation angle of the rear axle AB with respect to the x axis of the coordinate system is α , so the rotation angle of the whole car obtained by Eqs. is

$$d\alpha = \frac{d\theta \pi D}{i(b - c \frac{l \cos \theta(t)}{a})} \frac{l \cos \theta(t)}{a} \quad (2)$$

where i – Gear ratio,

D – Radius of the driving wheel 1, $D = 220mm$.

The coordinate matrix of the track of the driving wheel 1 in the coordinate system xoy is (x_A, y_A) , so the coordinate matrix of the track of the steering wheel 3 in the coordinate system xoy is

$$\begin{bmatrix} x_C \\ y_C \end{bmatrix} = \begin{bmatrix} x_A \\ y_A \end{bmatrix} + \begin{bmatrix} c & -b \\ b & c \end{bmatrix} \begin{bmatrix} \cos \alpha \\ \sin \alpha \end{bmatrix} \quad (3)$$

When the space of obstacles is 1000mm , $a = 50\text{mm}$, $b = 284\text{mm}$, $l = 27\text{mm}$. For the stability of running, the rear wheels are symmetrically arranged [6], and the gear ratio $i = 4$.

3. Error Analysis and Solution

3.1. Causes analysis of track error

The running track is mainly formed by the driving and driven wheels which are led by the steering wheel, and the main function of the driving and driven wheels is to provide the driving force. When the car runs at a certain speed, the steering wheel rotates with the steering shaft, and then, the moving direction of the car will change. In order to meet the theoretical requirement of rotation, the ultimate angles of the steering shaft within push and return travel need to be the same [7], so the error degree between ultimate angles within push and return travel is critical to the

consistency between practical and theoretical running track.

When the main structure and the assembly error is reasonable, the space of obstacles is set to be 1000mm . After several experiments, the running tracks can mainly be divided into the next four kinds.

(1) During the process of running, the track from the departure to the end changes with a sine curve. The mean curve of the whole track is linear and coincides with the center line of the racetrack. This track is the ideal one, as is shown in Fig. 3;

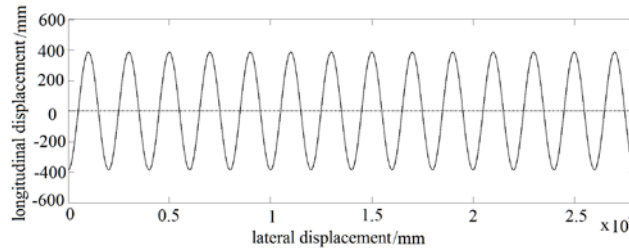


Fig. 3. Practical track 1

(2) During the process of running, the track from the departure to the end changes with sine curve. The mean curve of the whole track is linear and appears an angle γ_1 with the central line of the racetrack, as is shown in Fig. 4;

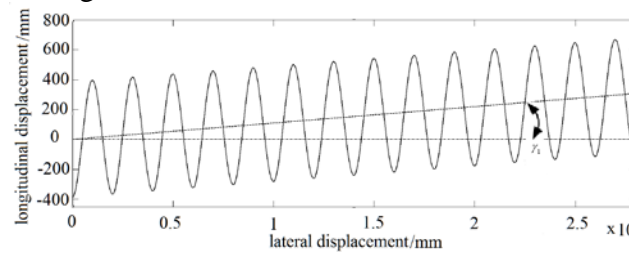


Fig. 4. Practical track 2

(3) During the process of running, the track from the departure to the end changes with a sine curve. The mean curve of the whole track is approximate to a section of symmetrical arc, and the line which connects the start and the end point of the arc coincides with the center line of the racetrack, as is shown in Fig. 5;

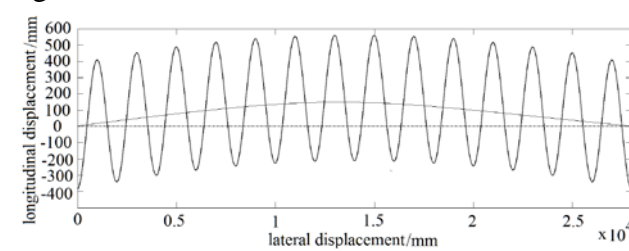


Fig. 5. Practical track 3

(4) During the process of running, the track from the departure to the end changes with a sine curve. The mean curve of the whole track is approximate to a section of symmetrical arc, and the line which connects the start and the end point of the arc appears an angle γ_2 with the central line of the racetrack, as is shown in Fig. 6;

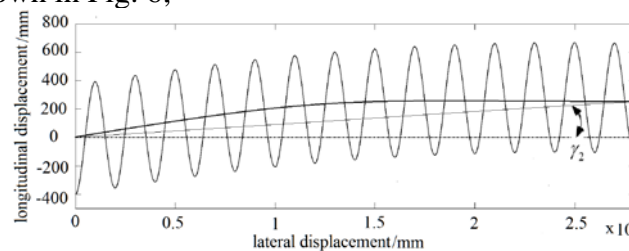


Fig. 6. Practical track 4

As mentioned above, in addition to the certain radian, the running track also has a feature of the overall rotation. As is shown in Fig. 3 and Fig. 4, Fig. 5 and Fig. 6.

To sum up, when the car departs normally, the deviation between the practical and the predicted track is also related to the error of departure angle besides the error between ultimate angles of the steering shaft within push and return travel, which is just the angular deflection between the center line of chassis and the center of racetrack.

3.2. Scheme of Adjustment

As for the error of departure angle, it will be decreased or even eliminated by special-designed departure device which takes the generatrix of the rear axle and the departure line for reference. However, the error between ultimate angles of the steering shaft within push and return travel is caused by lots of assembly errors. Because the push and the return motion of the steering shaft are mainly realized by the push of the crank, the angle error which is difficult to control can be turned into the easy-controlled adjustment quantity of the guide-bar $\Delta\epsilon$. The schematic diagram of the theoretical and practical ultimate angles of the rocker is shown in Fig. 7.

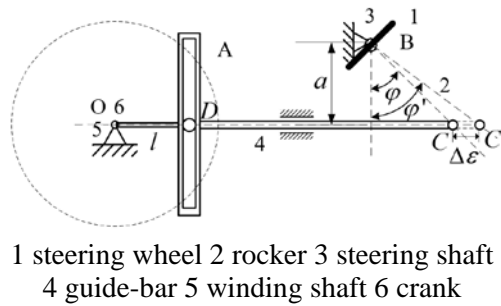


Fig. 7. Theoretical and practical ultimate angles of the rocker

So according to Eqs. (9), (10) and the introduced parameters above, the practical ultimate angle of the bar is

$$\varphi(t)_{push}' = \arctan \left[\frac{l \cos \theta(t) \pm \Delta\epsilon}{a} \right] \quad (4)$$

In order to ensure the accuracy of adjustment and the stability during running, the adjusting mechanism shown in Fig. 8 is applied in this paper.

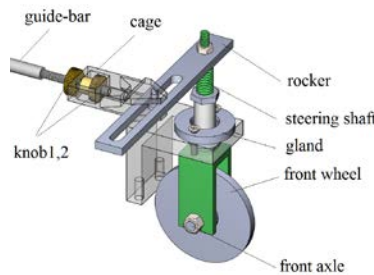


Fig. 8. Adjusting mechanism

The front of the guide-bar is screw pair whose pitch is P , and the adjustment quantity is $\Delta L = P/k$ per time. After the adjustment of guide-bar by adjusting knob 1 which is made of copper, the knob 2 will lock the guide-bar to ensure stability during running.

4. Simulation Analysis and Experimental Verification

The virtual prototype model of the car is established according to the related parameters before the simulation. In order to be the same with the practical running situation, some parameters of the kinematic pairs still need to be set with the combination of practical environment and related data.

4.1. Simulation Procedure

The car needs a larger torque due to overcoming the maximum static friction force[8,9] and then, it will run at a stable speed with a small acceleration after time t_0 . The torque provided by the winding shaft is approximated to be

$$T = \begin{cases} \xi mg \frac{d_0}{2} t & 0 \leq t \leq t_0 \\ \lambda T_0 + kt & t \geq t_0 \end{cases} \quad (5)$$

where ξ –Friction coefficient with the consideration of the friction loss of the winding shaft and pulley,

m –Weight of the heavy hammer,

d_0 –Diameter of the larger section of the winding shaft,

T_0 – Maximum driving torque,

λ – Coefficient of the driving torque,

k – Coefficient of the velocity increment.

According to the known parameters, the driving equation of running time t which is programmed by *STEP* function[10,11] is

Function

step(time,0,0,4,86.14)+step(time,4.1,0,4.7,-43.07)

+step(time,5,0,100,5.62)

Fig. 9 shows the curve of the running torque.

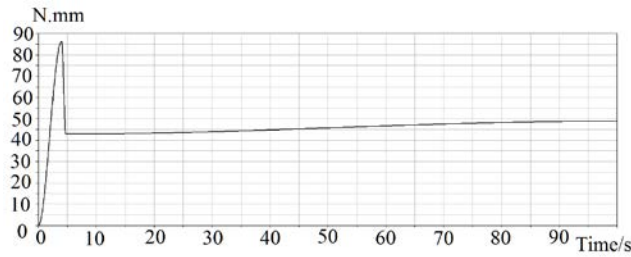


Fig. 9. Curve of torque

As to the revolute pairs where the deep groove ball bearings are applied, when their equivalent dynamical load $P \approx 0.1C$ and they are lubricated and run well, the friction coefficient $\mu = 0.0015 \sim 0.0022$ [12]. Because the load of the bearings is in the radial direction mainly, the friction coefficient μ takes the smaller one 0.0017 [13].

Then the related size parameters of the car are set according to the space of obstacles which is 1000mm. After the import of the model, the related parameters of the constraint and kinematic pairs will be set as mentioned above and then, the whole virtual prototype model is established.

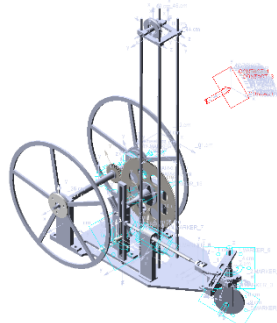


Fig. 10 Virtual prototype model

The adjustment quantity P is set to be 0.5mm. The variable quantity of ultimate angles of the

steering shaft within push travel and return travel approximates to be $0.448^\circ / P$. The simulation result is shown in Fig. 11.

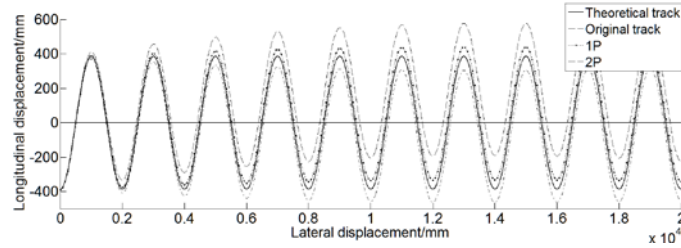


Fig. 11. Tracks of different total adjustment quantity (0.5mm)

Although the running track after the total adjustment quantity $1P$ in Fig. 11 has been approximated to the theoretical track a lot, there is still a large deviation between the practical and the theoretical track. With the increase of the running distance, the car may have been deviated from the racetrack before reaching the terminal point, so it is necessary to make the further adjustment.

P is reset to be $0.25mm$ again and the simulation is carried out on the basis of the running track whose total adjustment quantity is $1P$ in Fig. 11. The simulation result is shown in Fig. 12.

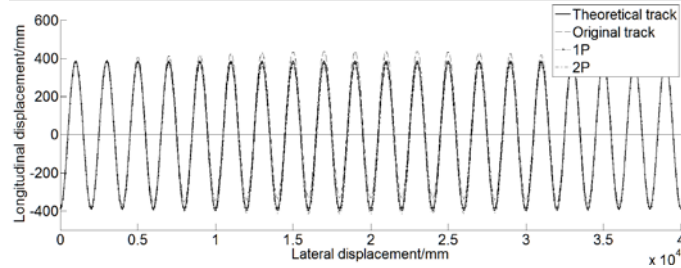


Fig. 12. Tracks of different total adjustment quantity (0.25mm)

When the total adjustment quantity is $1P$, the variable quantity of ultimate angles of the steering shaft within push travel and return travel approximates to be $0.222^\circ / P$, and the running track is in accordance with the theoretical almost. In Fig. 12, the running distance is $40000mm$ and the degree of divergence is too small to be taken into consideration, so the proper adjustment quantity of the guide-bar can be $0.25mm$. In consideration of the stiffness and the model of the linear bearing, the precise screw pair $M4 \times 0.25mm$ is taken as the final choice.

4.2. Experimental Verification

In order to verify the effectiveness of the virtual prototype model built above and the precise screw pair $M4 \times 0.25mm$, the physical prototype model which is improved based on the former one is built and shown in Fig. 13.



Fig. 13 Improved physical prototype model

When the track meets the requirements, the length of the crankshaft and the adjust quantity of the guide-bar and the knob are shown in the Table. 1.

Table 1 The experimental data.

Obstacle Distance(mm)	700	800	900	1000	1100	1200	1300
Crank(mm)	41.5	37	33	27	22.5	16.8	9
Adjustment(mm)	4	5	6	7	8	8	9
Fine Adjustment(mm)	0.75	0.5	0.25	0.5	0.12	0.5	0.25

According to the experiment dates, we find that with the decrease of the obstacles space, the crank length increases and the car gets more sensitive to the changes in guide-bar[14], even a tiny adjustment will cause a high deviation to the track. When the obstacles space becomes larger, the length of the crank is reduced, and the sensitivity is decreased. The result directly reflects in the actual angle of the push bar, which is in accordance with the formula (4). During the adjustment process, the 0.25mm quantity meets the minimum adjustment requirement, which greatly reduces the adjustment time.

After the optimization of structure and related parameters, the running track of carbon-free is in accordance with the theoretical almost. Finally, the car avoids 38 obstacles successfully and achieves a great grade.

5. Conclusions

(1) The mathematical model of car motion is built by the analytical method and the two main causes of the track deviation are concluded.

(2) By the premise of eliminating the error of departure angle, the error of rotation angle can be turned into the adjustment quantity of guide-bar. And an adjustment scheme which adjusts the length of guide-bar by screw pair is proposed to compensate the ultimate angle error of the steering shaft. The detailed structure is designed.

(3) The virtual prototype model of carbon-free car is established for track simulation. The simulation result shows that 0.25mm is the proper adjustment quantity and the following experiments verify the effectiveness and correctness of the proposed model and method.

References

- [1] ZENG Silong, WENG Huang, NI Boyang. Innovation design of the carbon-free car turning mechanism [J]. Silicon Valley, 2013, 10: 36-37.
- [2] LI Jie, XIE Liangxi, MA Zhao, CHEN Jianwen, ZHANG Yi, TIAN Zhixiang. Simulation and optimization of steering mechanism of carbon trolley track [J]. Mechanical Engineer, 2015, 7: 36-38.
- [3] WU Xinliang, LIU Jianchun, ZHENG Chaoyan. Design and manufacturing for gravity-driven and obstacle-free vehicle [J]. Journal of Machine Design, 2014, 10: 25-28.
- [4] ZOU Guangming, WANG Dongxiong, YIN Zhipeng, LIU Yuanjong, SHEN Huan. Study on the obstacle avoidance car based on incomplete gear rack mechanism for steering [J]. Mechanical & Electrical Engineering Technology, 2014, 43: 8-10, 26.
- [5] GUAN Wenfang. Model and simulation research of bond graph of sine mechanism [D]. Hunan, China, Central South University, 2011:9-11.
- [6] LIU Yang, JIANG Jiguang, XIE Chun. Innovative design of the carbon-free car fine-turning mechanism based on the trajectory analysis method [J]. Journal of Mechanical Transmission, 2015, 39(12): 83-86.
- [7] LI Licheng, XU Manlin, KE Chantgfu. Structural design for the S-shaped carbon-free vehicle [J]. Mechanical Research & Application, 2015, 3: 152-154.
- [8] WANG Liqing, CHEN Tieming. Mechanical design [M]. Harbin, Harbin Institute of Technology Press, 2009: 46-47.

- [9] Li Gang, Zhou Zhicheng, Yuan Hang, Zhang Darning, Wangchao. Sports car without carbon S-shaped turn improve the design study [J]. Automobile Applied Technology, 2014, 2: 14.
- [10] LI Qiujuan. Working stability analysis for dump truck based on ADAMS [D]. Hubei, China, Hubei University of Technology, 2009:31-32.
- [11] ZHANG Guoding. A model of impact Dynamics of multi-arm robots [J]. Mechanical Science and Technology, 1996, 15(1):57-56.
- [12] Zhang Dingguo. The Equations of External Impacted Dynamics between multi-rigid body system [J]. Applied Mathematics and mechanics, 1997.
- [13] Wu S-C, Haug EJ. A substructure technique for dynamic of flexible mechanical systems with contact-impact [J]. ASME J mech Des, 1990, 112:390-8.
- [14] FU Zhihe. Effect of center of gravity deviating to traveling stability of wheel engineering vehicle [J]. Construction Machinery, 2007, 3: 61-62.